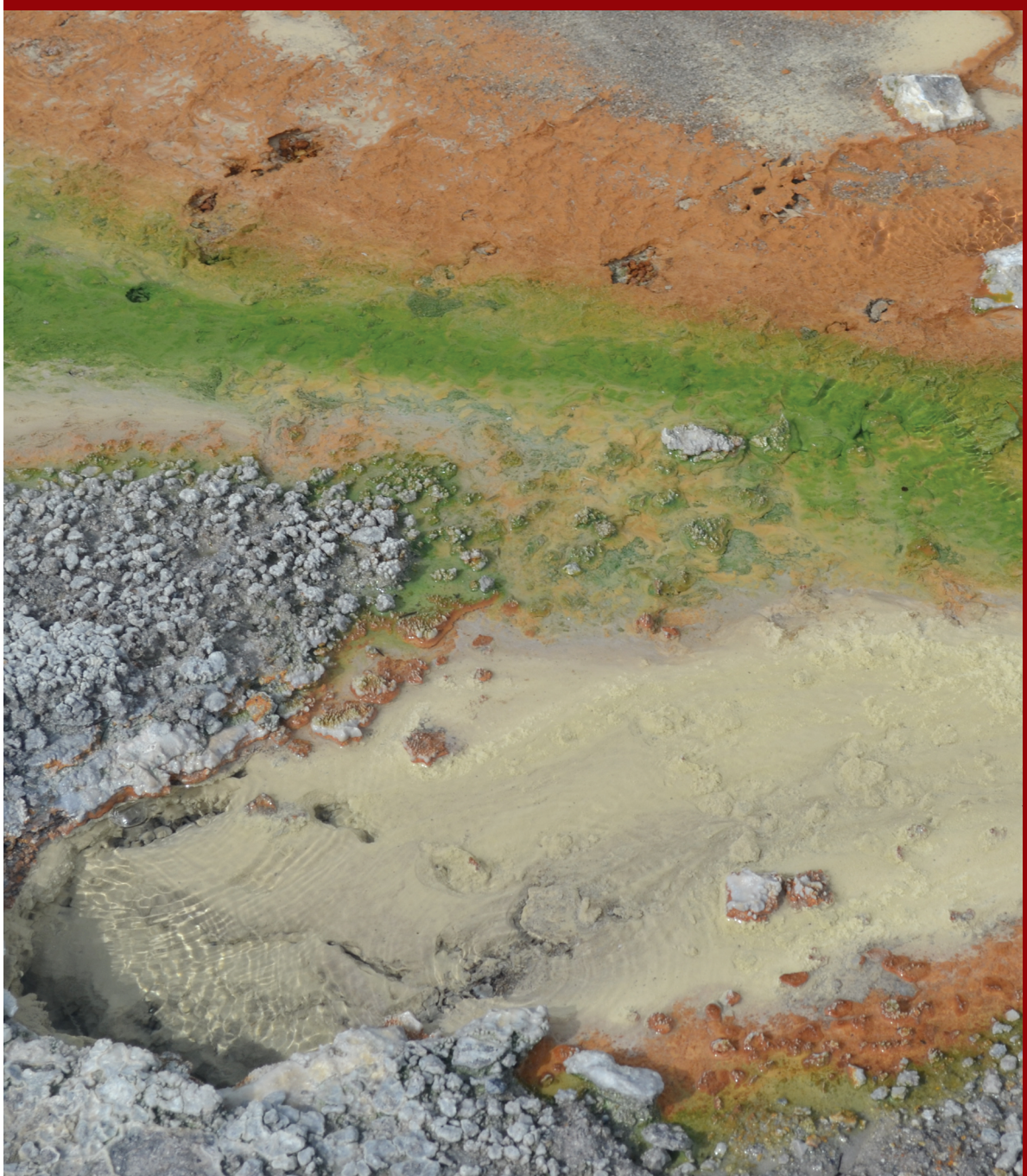
June 2018 • Volume 84 • Number 12

AEM

Applied and Environmental Microbiology



published twice monthly by

AMERICAN SOCIETY FOR MICROBIOLOGY

AMERICAN SOCIETY FOR MICROBIOLOGY | Applied and Environmental Microbiology®

GEOMICROBIOLOGY

Mechanisms of Mineral Substrate Acquisition in a Thermoacidophile

Maximiliano J. Amenabar,[a] Eric S. Boyd[a,b]

[a]Department of Microbiology and Immunology, Montana State University, Bozeman, Montana, USA
[b]NASA Astrobiology Institute, Mountain View, California, USA

ABSTRACT The thermoacidophile *Acidianus* is widely distributed in Yellowstone National Park hot springs that span large gradients in pH (1.60 to 4.84), temperature (42 to 90°C), and mineralogical composition. To characterize the potential role of flexibility in mineral-dependent energy metabolism in contributing to the widespread ecological distribution of this organism, we characterized the spectrum of minerals capable of supporting metabolism and the mechanisms that it uses to access these minerals. The energy metabolism of *Acidianus* strain DS80 was supported by elemental sulfur (S^0), a variety of iron (hydr)oxides, and arsenic sulfide. Strain DS80 reduced, oxidized, and disproportionated S^0. Cells growing via S^0 reduction and disproportionation did not require direct access to the mineral to reduce it, whereas cells growing via S^0 oxidation did require direct access, observations that are attributable to the role of H_2S produced by S^0 reduction/disproportionation in solubilizing and increasing the bioavailability of S^0. Cells growing via iron (hydr)oxide reduction did not require access to the mineral, suggesting that the cells reduce Fe(III) that is being leached by the acidic growth medium. Cells growing via oxidation of arsenic sulfide with Fe(III) did not require access to the mineral to grow. The stoichiometry of reactants to products indicates that cells oxidize soluble As(III) released from oxidation of arsenic sulfide by aqueous Fe(III). Taken together, these observations underscore the importance of feedbacks between abiotic and biotic reactions in influencing the bioavailability of mineral substrates and defining ecological niches capable of supporting microbial metabolism.

IMPORTANCE Mineral sources of electron donor and acceptor that support microbial metabolism are abundant in the natural environment. However, the spectrum of minerals capable of supporting a given microbial strain and the mechanisms that are used to access these minerals in support of microbial energy metabolism are often unknown, in particular among thermoacidophiles. Here, we show that the thermoacidophile *Acidianus* strain DS80 is adapted to use a variety of iron (hydro)oxide minerals, elemental sulfur, and arsenic sulfide to support growth. Cells rely on a complex interplay of abiologically and biologically catalyzed reactions that increase the solubility or bioavailability of minerals, thereby enabling their use in microbial metabolism.

KEYWORDS elemental sulfur reduction, elemental sulfur oxidation, elemental sulfur disproportionation, iron reduction, realgar oxidation, arsenic, Yellowstone, acidophile, ferric iron, thermophile

Microbial life in high-temperature hot-spring environments (>73°C) is supported by chemical sources of energy (1–4) supplied primarily by volcanic degassing (volatiles) and water-rock interactions (solutes and volatiles) (5–7). The amount of and variability in the composition of chemical sources of energy in hot springs are dependent on processes that take place deep in the subsurface as well as those that take

Received 7 February 2018 **Accepted** 2 April 2018

Accepted manuscript posted online 6 April 2018

Citation Amenabar MJ, Boyd ES. 2018. Mechanisms of mineral substrate acquisition in a thermoacidophile. Appl Environ Microbiol 84:e00334-18. https://doi.org/10.1128/AEM.00334-18.

Editor Robert M. Kelly, North Carolina State University

Copyright © 2018 American Society for Microbiology. All Rights Reserved.

Address correspondence to Eric S. Boyd, eboyd@montana.edu.

Downloaded from http://aem.asm.org/ on May 31, 2018 by MONTANA STATE UNIV AT BOZEMAN

place near the surface (8). The subsurface process of decompressional boiling of ascending hydrothermal fluids and separation of this fluid into a vapor phase and a liquid phase can markedly influence the geochemical composition of hydrothermal fluids (9–12). Partitioning of hydrogen sulfide (H_2S) into the vapor phase, interaction of this H_2S-enriched vapor with infiltrating near-surface oxygen (O_2)-rich meteoric fluids, and aerobic oxidation of H_2S to elemental sulfur (S^0) and ultimately to sulfuric acid are thought to drive the development of acidic spring waters (9, 11–13). In turn, these acidic waters are more effective in leaching minerals from subsurface bedrock than circumneutral to alkaline liquid-phase-influenced waters, which can further influence the geochemical composition of fluids and the availability of electron donors and acceptors (9, 11, 14, 15; M. R. Lindsay, M. J. Amenabar, K. M. Fecteau, R. V. Debes, M. C. F. Martins, K. E. Fristad, H. Xu, T. M. Hoehler, E. L. Shock, and E. S. Boyd, submitted for publication).

Variation in the availability of electron donors and acceptors, in both soluble and insoluble (mineral) forms, drives variation in the taxonomic and functional compositions of chemotrophic hot-spring communities (13, 16–20; Lindsay et al., submitted). Redox-active minerals that can support microbial metabolism in hot-spring environments include S^0 (16, 21–23) that is formed from the incomplete near-surface oxidation of H_2S (8, 13, 21, 24, 25). S^0 is generally more common in acidic hot springs (20, 22), since these springs are influenced to a greater degree by vapor-phase input that is enriched in H_2S relative to liquid-phase input (12). Numerous reports have demonstrated the use of S^0 as an electron donor (26–28) or as an electron acceptor (22, 23, 27–29) in supporting the metabolism of thermophilic microorganisms in hot-spring environments. Far less is known of the role of S^0 when it serves as both electron donor and electron acceptor for microbial metabolism in a process termed S^0 disproportionation (30–35). To our knowledge, only one thermophilic bacterium with the ability to disproportionate S^0 has been described to date (33). All other reported organisms capable of growth via S^0 disproportionation are mesophilic neutrophiles within the bacterial domain (30–35).

In addition to S^0, minerals capable of supporting microbial metabolism that are common in hot springs include a variety of iron (hydr)oxides (21, 25, 36–40), which result from the near-surface oxidation of ferrous iron [Fe(II)] with oxygen (41, 42). Fe(II) and ferric iron [Fe(III)] are more soluble in acidic waters (43) and are enriched in many acidic hot springs (see Fig. S1B and C, respectively, in the supplemental material) (15). As such, many acidic springs have iron (hydr)oxide depositional zones resulting from oxidation of Fe(II) (21, 25, 41, 42, 44). Despite these observations, only a few thermoacidophiles have been shown to couple Fe(III) reduction to growth under high-temperature acidic conditions (27, 45–47). Moreover, it is not known whether these thermoacidophiles reduce solid-phase iron (hydr)oxides or whether they reduce Fe(III) released by acid-promoted dissolution of these minerals.

Other redox-active minerals that are common in hot-spring environments include arsenic sulfides such as realgar (α-As_4S_4) and orpiment (As_2S_3) that can result from the precipitation of soluble arsenic (As) by H_2S (48, 49). Soluble As (see Fig. S2A, B, and C in the supplemental material) (15) and arsenic sulfides have been detected across a broad range of hot springs with variable pH (49–52). Numerous studies have shown the ability of microorganisms to oxidize and reduce soluble As in hot-spring environments and couple this activity to growth (25, 42, 53–55). However, we are unaware of any microorganism, thermophilic or otherwise, that has been demonstrated to oxidize mineral forms of As, such as α-As_4S_4 or As_2S_3, and couple this to growth.

We previously isolated a thermoacidophilic crenarchaeote belonging to the *Acidianus* genus from an acidic hot spring known as "Dragon Spring," Norris Geyser Basin (NGB), Yellowstone National Park (YNP), Wyoming, USA, and designated this strain DS80 (27). Our prior partial physiological characterization indicates that strain DS80 displays versatility in lithotrophic energy metabolism involving hydrogen (H_2) or S^0 as electron donors and S^0 or soluble/mineral forms of Fe(III) as electron acceptors (27; M. J. Amenabar, D. R. Colman, S. Poudel, E. E. Roden, and E. S. Boyd, submitted for publica-

Downloaded from http://aem.asm.org/ on May 31, 2018 by MONTANA STATE UNIV AT BOZEMAN

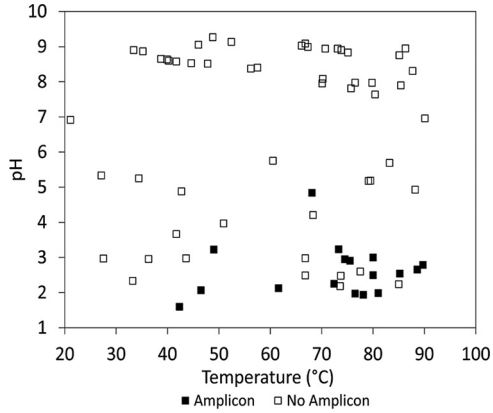


FIG 1 The presence (black squares) or absence (white squares) of *Acidianus* sp. *sor* amplicons in DNA extracts from sediments collected from 73 hot springs in Yellowstone National Park plotted as a function of the pH and temperature of those springs.

tion). The demonstrated ability of this strain to couple the iron, sulfur, hydrogen, and carbon cycles in overlapping ways in addition to the global distribution of *Acidianus* in thermal environments (56) suggests that the activity of strain DS80 is likely to have an important role in modulating the geochemistry of hot-spring environments. However, aside from Fe(III) and S^0, the spectrum of mineral-based substrates that can support growth of DS80 was not determined. Thus, despite the ability of strain DS80 to respire several solid-phase Fe(III) and S^0 minerals, key questions remain unanswered, including how these cells access these mineral substrates to support their metabolism. Specifically, it is not known how cells couple redox reactions that involve multiple solid-phase minerals when they serve as electron donor and acceptor [e.g., coupling S^0 oxidation to iron (hydr)oxide reduction].

In this study, we determined the distribution of strain DS80 across pH, temperature, and mineralogical gradients in 73 hot springs in YNP. The widespread distribution of this strain in hot-spring sediments that contained various combinations of S^0, iron (hydr)oxides, and arsenic sulfides prompted additional physiological studies aimed at further characterizing the flexibility in the mineral-dependent energy metabolism of strain DS80. Specifically, we aimed to determine which of the solid-phase minerals that are commonly detected in acidic hot-spring environments [i.e., S^0, iron (hydr)oxides, and α-As_4S_4] can support growth of DS80. Moreover, we aimed to characterize the mechanisms involved in accessing these mineral substrates. The results suggest that flexibility in the mineral-dependent metabolism of strain DS80, combined with feedbacks between abiotic and biotic processes that increase the bioavailability of minerals, may contribute to the widespread distribution of this strain in low-pH hot-spring habitats with differing mineralogical compositions.

RESULTS

Distribution of *Acidianus* spp. in YNP hot springs. Primers specific for the amplification of *sor* from *Acidianus* spp. were used to determine the distribution of this gene as a proxy for *Acidianus* in sediments sampled from 73 hot springs that spanned a pH gradient from 1.60 to 9.27 and a temperature range from 21.1°C to 90.1°C. *sor* amplicons were detected in DNA extracts from 18 of the 73 samples, all of which had acidic pH (<4.9) and elevated temperatures (>42°C) (Fig. 1). The 18 samples were collected from hot springs from geographically distinct locations in YNP, including the One Hundred Springs Plain area of NGB, Crater Hills (CH), Geyser Creek, the Obsidian Pool area, the Sylvan Spring area, and the Nymph Lake (NL) area. These sediments visibly contained various combinations of S^0, iron (hydr)oxides, and/or arsenic sulfides (e.g., see Fig. S3 in the supplemental material). This suggested the potential use of these minerals by *Acidianus* spp. Moreover, these results indicate that *Acidianus* spp.

Downloaded from http://aem.asm.org/ on May 31, 2018 by MONTANA STATE UNIV AT BOZEMAN

have a broad ecological distribution that potentially spans a pH gradient of 1.60 to 4.84, a temperature gradient of 42.3°C to 89.7°C, and a gradient in the availability of redox-active mineral substrates.

Since *sor* amplicons were not sequenced, we cannot confirm their relationship to strain DS80. However, to confirm that *Acidianus* spp. were present and viable in YNP springs where *sor* amplicons were detected, dilution-to-extinction serial enrichments were conducted with sediments sampled from a subset of springs using anoxic mineral salts growth medium amended with H_2 as an electron donor and S^0 as an electron acceptor with CO_2 as a carbon source. Positive enrichments were obtained from sediments sampled from all 5 of the springs where enrichments were performed. These include an arsenic hydrous ferric oxide- and S^0-rich spring in NGB informally called "Dragon Spring" (25) (Fig. S3A), two unnamed S^0- and Fe-rich springs in NGB (Fig. S3B and C), an S^0-rich spring in NL informally called "NL_2" (20) (Fig. S3D), and an S^0-rich spring in CH informally called "Alice Spring" (57) (Fig. S3E). The pH, temperature, global positioning system coordinates, and images of each spring are reported in Fig. S3. Serial passage of these enrichments, in combination with dilution to extinction, resulted in cultures with a single morphotype. Sequencing of 12 archaeal clones from each of the five cultures yielded closely related 16S rRNA gene phylotypes. 16S rRNA gene sequences from the 5 cultures ranged from being 99% to 100% identical to the 16S rRNA gene from *Acidianus hospitalis* (accession number CP002535). We used the culture isolated from Dragon Spring (NHSP042), designated strain DS80 (27; Amenabar et al., submitted), which has a 16S rRNA gene (accession number KX608545) that is 100% identical to that from *A. hospitalis*, in the physiological studies described below.

Despite the sequence identity of the 16S rRNA gene and a close phylogenomic relationship between strain DS80 and *A. hospitalis* (Amenabar et al., submitted), key differences exist between their genomes that likely drove their divergence and influence their respective ecologies. Among these are genes encoding an uptake [NiFe]-hydrogenase and a sulfur reductase complex in the strain DS80 genome but not in the *A. hospitalis* genome (58). The presence of these genes in the DS80 genome is consistent with the ability of strain DS80 to conserve energy with the H_2/S^0 redox couple (27; Amenabar et al., submitted).

Surface requirement for mineral-dependent growth. The abilities of minerals such as S^0, iron (hydr)oxides, and arsenic sulfides to support growth and the requirement for access to mineral surfaces by strain DS80 when these minerals are supplied as electron donors or acceptors, or both, were determined. Cells of strain DS80 were capable of coupling S^0 reduction with H_2 as the electron donor under autotrophic growth conditions, and this reaction supported cell growth (Fig. 2A and B). H_2/S^0-grown DS80 cells reduced S^0 when it was sequestered in dialysis tubing with different pore sizes, indicating that physical contact with bulk solid-phase S^0 was not necessary. Moreover, rates of growth and activity were dependent on the dialysis membrane pore size, with higher rates detected when S^0 was sequestered in dialysis membranes with larger pores. This suggests that the sulfur compound that is serving as an electron acceptor exhibits a distribution of particle sizes, which is similar to observations made previously for the thermoacidophilic sulfur reducer *Acidilobus sulfurireducens* (23). This interpretation is further supported by previous abiotic experiments that showed that S^0 nanoparticles coarsen rapidly over short periods of time (59) (see Discussion for more details).

Specific growth yields, or the number of cells produced per mole of product produced, when strain DS80 was cultivated with direct access to S^0 or when S^0 was sequestered in dialysis membranes were not significantly different (Table 1). Generation times, calculated during log-phase growth, were 25.7 $\pm$ 5.7 h when cells were provided access to S^0, whereas they were 40.4 $\pm$ 2.2 h and 178.9 $\pm$ 77.3 h when S^0 was sequestered in dialysis tubing with pore sizes of 12 to 14 kDa and 6 to 8 kDa, respectively. It is not clear that cells grown with S^0 sequestered in dialysis membranes with the restricted pore size of 6 to 8 kDa entered log-phase growth, which may

Downloaded from http://aem.asm.org/ on May 31, 2018 by MONTANA STATE UNIV AT BOZEMAN

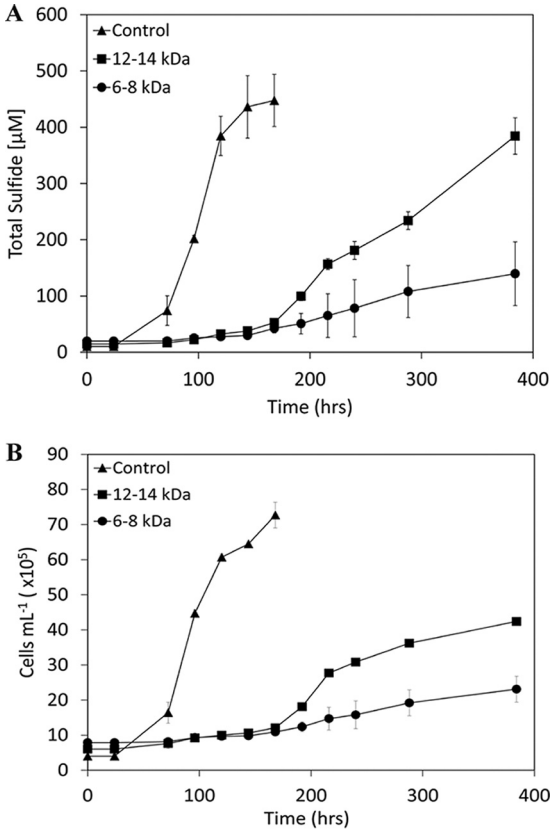


FIG 2 Sulfide concentrations (A) and cell concentrations (B) in cultures of strain DS80 grown autotrophically with H_2 as electron donor and S^0 as electron acceptor. S^0 was provided in the bulk medium (control) or was sequestered in dialysis membranes (pore sizes of 12 to 14 kDa or 6 to 8 kDa) to prevent physical contact with the bulk mineral.

indicate that rates of cell death nearly balance rates of cell production in these cultures. Moreover, the final cell densities were 41% and 68% lower when S^0 was sequestered in dialysis tubing with pore sizes of 12 to 14 kDa and 6 to 8 kDa, respectively, than when cultures were grown with S^0 in the bulk medium. These results suggest that the sulfur compound that supports growth of DS80 is soluble and that this compound limits growth.

Strain DS80 was capable of coupling S^0 oxidation with Fe(III) as ferric sulfate serving as electron acceptor under autotrophic growth conditions, and this reaction supported production of cells (Fig. 3A and B). However, growth was not observed when cells were grown with S^0 and Fe(III) when S^0 was sequestered in dialysis tubing. Thus, in contrast to cells reducing S^0, cells oxidizing S^0 apparently require direct physical contact with the mineral to catalyze its oxidation.

Strain DS80 was capable of S^0 disproportionation under autotrophic growth conditions, and this reaction supported production of cells (Fig. 4A to C). The concentration of total sulfide, the concentration of sulfate, and the density of cells increased concurrently in cultures of strain DS80 grown with S^0 as the sole electron donor and acceptor. S^0 was disproportionated to hydrogen sulfide (H_2S) (4.95 $\pm$ 1.12 μmol at the end of exponential phase) and sulfate (SO_4^{2-}) (1.36 $\pm$ 0.10 μmol at the end of exponential phase) at a stoichiometry close to 3 mol sulfide (3.67 $\pm$ 1.05) per mol of sulfate produced. This stoichiometry agrees with that predicted from the equation $4S^0 + 4H_2O \rightarrow SO_4^{2-} + 3H_2S + 2H^+$.

Cells growing via S^0 disproportionation, like those growing via S^0 respiration, did not require direct physical contact with the mineral to catalyze its simultaneous oxidation to SO_4^{2-} and reduction to H_2S (Fig. 4A to C). The generation time (calculated during

Downloaded from http://aem.asm.org/ on May 31, 2018 by MONTANA STATE UNIV AT BOZEMAN

TABLE 1 Growth yields of strain DS80 cultivated in base salts medium at 80°C and pH 3.0[a]

Growth condition	Sequestered compound[b]	Direct (control) or indirect (membrane pore size, kDa) access to mineral	Growth yield (cells/pmol product)[c]	Generation time (h)
$S^0 + H_2 \rightarrow H_2S$	S^0	Control	12.0 ± 1.0	25.7 ± 5.7
		12–14	12.4 ± 0.4	40.4 ± 2.2
		6–8	15.0 ± 3.7	178.9 ± 77.3
$S^0 + 6Fe^{3+} + 4H_2O \rightarrow 6Fe^{2+} + HSO_4^- + 7H^+$	S^0	Control	7.3 ± 0.8	28.6 ± 0.2
		12–14	NG[e]	NG
		6–8	NG	NG
$4S^0 + 4H_2O \rightarrow SO_4^{2-} + 3H_2S + 2H^+$ (disproportionation)	S^0	Control	14.0 ± 4.2	23.6 ± 1.0
		12–14	14.6 ± 2.2	47.2 ± 1.8
		6–8	9.0 ± 0.8	112.3 ± 5.6
$H_2 + 2Fe^{3+}$ (ferrihydrite)[d] $\rightarrow 2Fe^{2+} + 2H^+$	Ferrihydrite	Control	3.4 ± 1.3	74.8 ± 2.8
		12–14	2.7 ± 0.5	156.8 ± 37.8
		6–8	3.9 ± 0.5	121.2 ± 57.7
α-$As_4S_4 + 20Fe^{3+} \rightarrow 4As^{5+} + 4S^0 + 20Fe^{2+}$	α-As_4S_4	Control	6.1 ± 1.3	61.1 ± 6.8
		12–14	4.6 ± 0.4	73.0 ± 3.0
		6–8	4.7 ± 1.1	76.0 ± 1.7

[a]Cells were grown autotrophically with H_2, S^0, or realgar (α-As_4S_4) as an electron donor and S^0, Fe(III) (as ferric sulfate), or ferrihydrite as an electron acceptors or with S^0 serving as both electron donor and acceptor (S^0 disproportionation), as specified. S^0, α-As_4S_4, and ferrihydrite were provided in the bulk medium (control) or were sequestered in dialysis membranes with different pore sizes (pore sizes of 12 to 14 kDa or 6 to 8 kDa) to prevent physical contact with the bulk mineral. Reported values represent the average and standard deviation from triplicate biological replicates.

[b]Substrate that was sequestered in dialysis tubing during growth.

[c]Growth yields are reported as cells per picomole H_2S ($S^0 + H_2$ growth condition), cells per picomole of Fe^{2+} ($S^0 + Fe^{3+}$ and $H_2 + Fe^{3+}$ growth conditions), cells per picomole of H_2S (S^0 disproportionation growth condition), or cells per picomole of As^{5+} (α-$As_4S_4 + Fe^{3+}$ growth condition).

[d]The formula for ferrihydrite is indeterminate, as its water content is variable and its basic crystal structure and physical properties remain controversial (90).

[e]NG, no growth.

log-phase growth) of cultures disproportionating S^0 when provided direct access to the mineral was 23.6 ± 1.0 h, whereas it was 47.2 ± 1.8 h and 112.3 ± 5.6 h when S^0 was sequestered in dialysis membranes with pore sizes of 12 to 14 kDa and 6 to 8 kDa, respectively (Table 1). Like for cells reducing S^0, the decrease in growth rate when S^0 was sequestered in dialysis membranes with smaller pore sizes suggest that the soluble sulfur compound that serves as electron acceptor and electron donor exhibits a size distribution.

Cells of strain DS80 reduced Fe(III) with H_2 as an electron donor under autotrophic growth conditions, and this reaction supported cell production. Cells grew with ferrihydrite sequestered in dialysis membranes (Fig. 5A and B), indicating that DS80 cells do not require direct access to this solid-phase mineral to use it as an electron acceptor. However, differences in growth kinetics and Fe(III) reduction activity were observed when cells were allowed direct contact with ferrihydrite compared to when ferrihydrite was sequestered in dialysis membranes. While the growth yield, or the amount of iron reduced per cell produced, did not vary significantly between growth conditions (all P values were >0.05) (Table 1), cells provided with direct access to ferrihydrite exhibited log-phase growth. In contrast, cultures grown with ferrihydrite sequestered in dialysis membranes did not appear to enter a log phase of growth, which may be due to limited availability of Fe(III). Like for cells growing with sequestered S^0, this may indicate that rates of cell death nearly balance those of cell production in cultures provided with sequestered ferrihydrite.

The generation time (calculated during log-phase growth) of cultures provided direct access to ferrihydrite was 74.8 ± 2.8 h, whereas the generation times of cultures grown with ferrihydrite sequestered in dialysis tubing with a pore size of 12 to 14 kDa or 6 to 8 kDa were 156.8 ± 37.8 h and 121.2 ± 57.7 h, respectively. The observation that the rates of iron reduction and generation times of cultures provided with ferrihydrite sequestered in dialysis tubing with a pore size of 12 to 14 kDa or 6 to 8 kDa were not significantly different ($P = 0.32$) indicates that the soluble form of Fe(III) that is being reduced does not exhibit a size distribution over this size range.

Preliminary experiments showed that the oxidation of soluble As(III) (supplied as $NaAsO_2$) supported growth of DS80 growth under aerobic and anaerobic conditions

Downloaded from http://aem.asm.org/ on May 31, 2018 by MONTANA STATE UNIV AT BOZEMAN

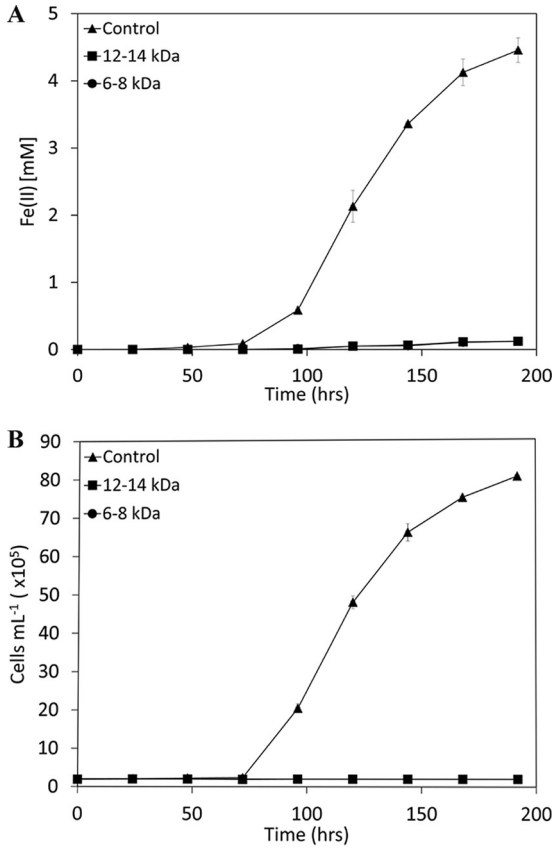


FIG 3 Fe(II) concentrations (A) and cell concentrations (B) in cultures of strain DS80 cultivated autotrophically with S^0 as electron donor and Fe(III) (provided as ferric sulfate) as electron acceptor. S^0 was provided in the bulk medium (control) or was sequestered in dialysis membranes (pore sizes of 12 to 14 kDa or 6 to 8 kDa) to prevent physical contact with the bulk mineral.

with Fe(III) as an electron acceptor (data not shown). This observation, in addition to qualitative (visual) evidence for the presence of arsenic sulfide minerals in spring sediments where *Acidianus* spp. were detected (Fig. 1) and where they were isolated (Fig. S3), prompted studies aimed at determining whether cells could use arsenic sulfides such as realgar (α-As_4S_4) as an electron donor. Autotrophic growth was observed when cultures were provided with α-As_4S_4 as an electron donor and Fe(III) (supplied as ferric sulfate) as an electron acceptor (Fig. 6A, B, and C). Cells were not able to grow with α-As_4S_4 as an electron donor and O_2 as an electron acceptor under autotrophic conditions (data not shown). With Fe(III) as an electron acceptor, cells were capable of growth when α-As_4S_4 was sequestered in dialysis membranes. This indicates that DS80 cells do not require direct access to this solid-phase mineral to use it as an electron donor. Growth yields, or the number of cells produced per mole of As(V) produced, when strain DS80 was cultivated with direct access to α-As_4S_4 or when α-As_4S_4 was sequestered in dialysis membranes with different pore sizes were not significantly different (Table 1). Generation times (calculated during log-phase growth) were 61.1 $\pm$ 6.8 h when cells were provided direct access to α-As_4S_4, whereas they were 73.0 $\pm$ 3.0 h and 76.0 $\pm$ 1.7 h when α-As_4S_4 was sequestered in dialysis tubing with pore sizes of 12 to 14 kDa and 6 to 8 kDa, respectively. The observation that rates of α-As_4S_4 oxidation and generation times were not significantly different ($P = 0.31$ and 0.12, respectively) in cultures provided with α-As_4S_4 sequestered in dialysis tubing with a pore size of 12 to 14 kDa or 6 to 8 kDa indicates that the soluble form of As that is being oxidized by DS80 and that is supporting growth does not exhibit a size distribution over the range tested.

Downloaded from http://aem.asm.org/ on May 31, 2018 by MONTANA STATE UNIV AT BOZEMAN

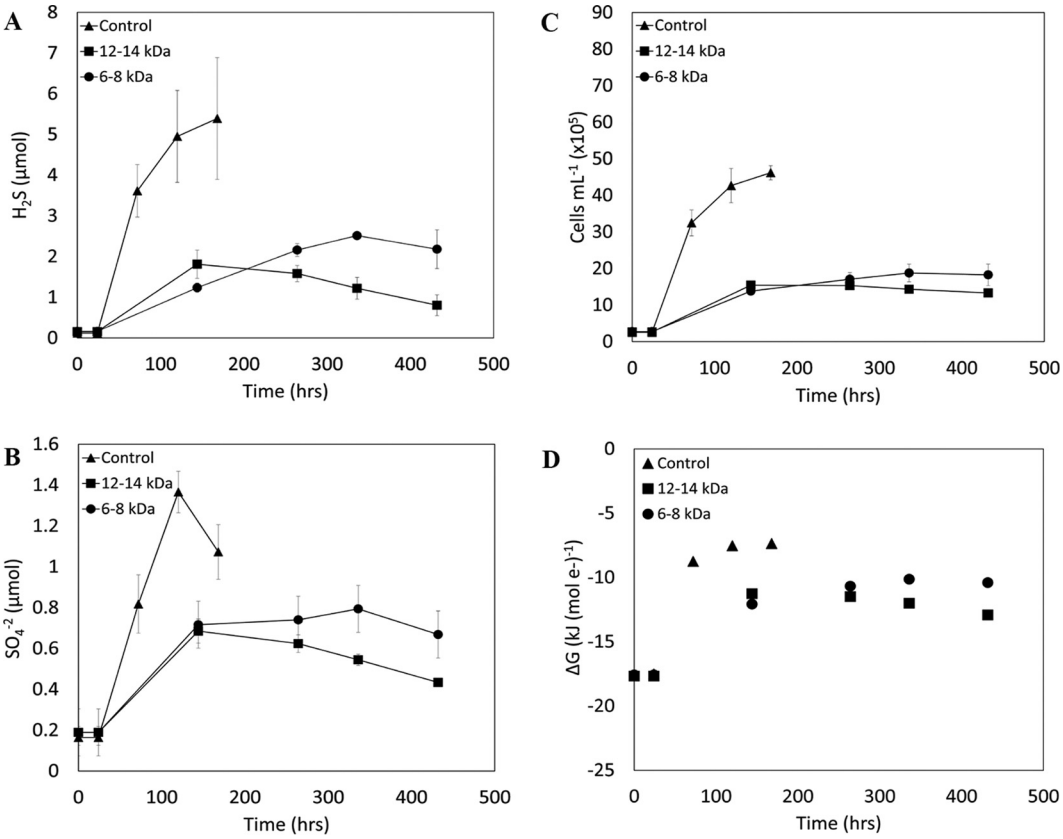


FIG 4 Sulfide concentrations (A), sulfate concentrations (B), cell concentrations (C), and available Gibbs free energy (Δ*G*) per mole of electrons transferred (D) in cultures of strain DS80 grown autotrophically with S^0 provided as electron donor and acceptor (S^0 disproportionation). S^0 was provided in the bulk medium (control) or was sequestered in dialysis membranes (pore sizes of 12 to 14 kDa or 6 to 8 kDa) to prevent physical contact with the bulk mineral.

Abiotic controls containing α-As_4S_4 and Fe(III) in cultivation medium showed moderate levels of Fe reduction, as indicated by production of Fe(II), and As oxidation, as indicated by As(V) production (see Fig. S4 in the supplemental material). However, the levels of production of both chemical species were significantly lower than for biological controls (Fig. 6A and B). This suggests the possibility that cells were oxidizing As(II) released by the abiotic oxidation of α-As_4S_4 by Fe(III). Importantly, neither SO_4^{2-} nor H_2S was detected in abiotic and biotic experiments (data not shown). This suggests that the sulfur that was released via the oxidation of α-As_4S_4 (by either biotic or abiotic mechanisms) likely ended up in the form of S^0. This suggestion is made since other intermediate forms of sulfur that could have been produced, such as thiosulfate, polysulfides, or polythionites, are unstable in acidic solutions and tend to degrade to form S^0 and sulfite, the latter of which is also unstable and oxidizes to SO_4^{2-} (8). The stoichiometry of oxidation of As(II) in α-As_4S_4 via Fe(III) (Table 1) should result in production of 1 mol As(V) and 5 mol Fe(II) if the reaction proceeds as written, with S^0 forming as a metastable product during oxidation of sulfide and As(II) released during oxidation of the sulfide mineral subsequently being oxidized to As(V). The observed stoichiometry of the products As(V) and Fe(II) at the end of exponential phase was 5.93 $\pm$ 1.04, which is within statistical error of the predicted stoichiometry (Table 1).

DISCUSSION

Strain DS80 was capable of growth with mineral sources of oxidant and/or reductant in the form of S^0, a variety of iron (hydr)oxides (ferrihydrite, goethite, and hematite [see Fig. S5 in the supplemental material]), and an arsenic sulfide (α-As_4S_4), consistent with the presence of these minerals in the hot springs from which DS80 and closely related

Downloaded from http://aem.asm.org/ on May 31, 2018 by MONTANA STATE UNIV AT BOZEMAN

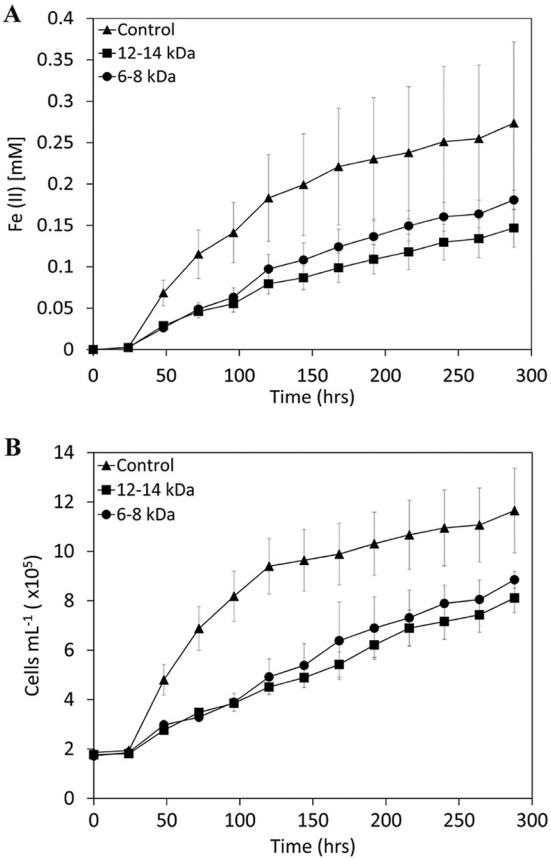


FIG 5 Fe(II) concentrations (A) and cell concentrations (B) in cultures of strain DS80 grown autotrophically with H_2 as electron donor and ferrihydrite as electron acceptor. Ferrihydrite was provided in the bulk medium (control) or was sequestered in dialysis membranes (pore sizes of 12 to 14 kDa or 6 to 8 kDa) to prevent physical contact with the bulk mineral. Note the scale difference in the *y* axis of panel B with respect to other growth conditions.

Acidianus (*Sulfolobales*) strains have been isolated (e.g., Dragon Spring [21, 25], NL_2 [20], and Alice Spring [57]). Previous studies have shown that members of the *Sulfolobales* are capable of using a variety of minerals to support metabolism; however, most of these studies focused on the role of strains in the oxidative dissolution of sulfidic ore minerals of economic interest (pyrite, sphalerite, and chalcopyrite) or the oxidation of S^0 (28). Just a few thermoacidophiles, including strain DS80 (27), *Acidianus manzaensis* (45), *Acidianus copahuensis* (47), "*Candidatus* Aciduliprofundum boonei" (60), *Sulfolobales* strain MK5, and *Acidicaldus* strain MK6 (46), have been shown to reduce soluble Fe(III) and couple this to growth. However, only *Acidianus manzaensis* (45), *Sulfolobales* strain MK5, *Acidicaldus* strain MK6 (45), and *Acidianus* strain DS80 (27) have been shown to reduce iron minerals at high temperature and low pH.

The ability of strain DS80 to oxidize As(III) is consistent with the presence of *aioAB* genes encoding the arsenite oxidase in the DS80 genome (Amenabar et al., submitted). Homologs of these genes have been previously reported in the genomes of other members of the *Acidianus* genus, including *A. hospitalis* (58) and *A. copahuensis* (47, 61). This study reports a thermoacidophile capable of oxidizing α-As_4S_4, either directly or indirectly, to support growth. Despite the broad range of YNP hot springs where soluble arsenic (see Fig. S2A, B, and C in the supplemental material) (15) and arsenic sulfides have been detected, arsenic-related geomicrobiology studies have focused largely on the oxidation of soluble forms of As in these environments (25, 42, 53–55). Field studies have demonstrated biological arsenic oxidation in an acidic hot spring from YNP (25), and follow-on studies successfully isolated a *Hydrogenobaculum* (*Aquificales*) strain capable of oxidizing soluble arsenite (53). The presence of microorganisms

Downloaded from http://aem.asm.org/ on May 31, 2018 by MONTANA STATE UNIV AT BOZEMAN

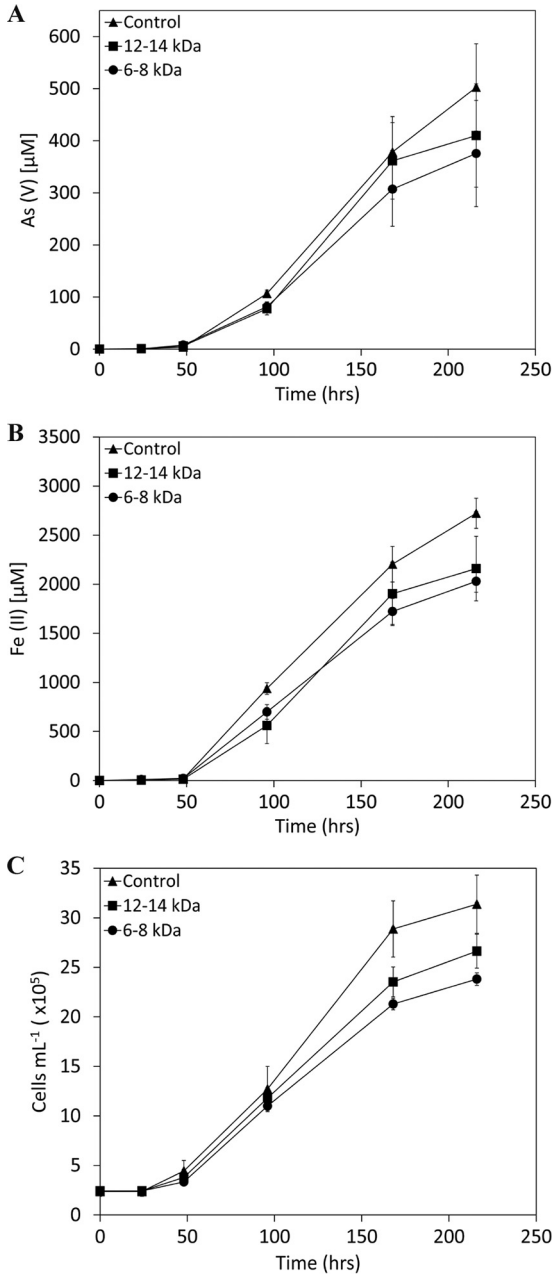


FIG 6 As(V) concentrations (A), Fe(II) concentrations (B), and cell concentrations (C) in cultures of strain DS80 grown autotrophically with realgar (α-As_4S_4) as electron donor and Fe(III) (provided as ferric sulfate) as electron acceptor. Realgar was provided in the bulk medium (control) or was sequestered in dialysis membranes (pore sizes of 12 to 14 kDa or 6 to 8 kDa) to prevent physical contact with the bulk mineral. Note the scale difference in the *y* axis of panel C with respect to other growth conditions.

capable of metabolizing arsenic compounds, including insoluble arsenic sulfides, suggests a role for biology (including strain DS80) in modulating the oxidation state and mobility of this metal in geothermal environments.

Strain DS80 was shown to couple S^0 disproportionation to growth, revealing the occurrence of this metabolic process in both an archaeon and an acidophile. The demonstrated ability to reduce, oxidize, and disproportionate S^0 suggests that strain DS80 is well adapted to use this mineral to support metabolism. This observation, combined with the ability of this strain to use iron and arsenic minerals, potentially explains its widespread distribution across numerous springs with various assemblages of minerals. Arguably, the

Downloaded from http://aem.asm.org/ on May 31, 2018 by MONTANA STATE UNIV AT BOZEMAN

diverse assemblage of minerals capable of supporting growth of DS80 is comparable to those of *Geobacter* spp. and *Shewanella* spp., the bacterial models for understanding the mechanisms of mineral reduction/oxidation in microbial metabolism (36, 62–65).

The demonstrated use of multiple minerals to support metabolism of DS80 prompted experiments aimed at understanding mechanisms for how these cells access minerals during growth. Dialysis membranes were used to limit the access of cells to the surfaces of S^0, iron, and arsenic sulfide minerals during growth. Like the thermoacidophile *A. sulfurireducens* (23), strain DS80 did not require direct access to S^0 to use it as an electron acceptor (Fig. 2A and B). It was previously suggested that S^0-reducing *A. sulfurireducens* cells were using a more soluble form of S^0 (nanoparticulate S^0) that existed in a range of particle sizes (23). This nanoparticulate S^0 was shown to form through a series of biological/abiological feedbacks, whereby H_2S resulting from the biological reduction of S^0 generates soluble linear chains of polysulfides (S_x^{2-} where *x* represents 3 to 6 S atoms) through abiotic nucleophilic attack on bulk (stacked) S_8^0 rings. The S_x^{2-} rapidly disproportionates abiotically under the acidic conditions of the cultivation medium, yielding soluble S_8 molecular rings (denoted as S^0 here) that rapidly aggregate or coarsen, reaching average particle diameters of 400 nm within several minutes of their disproportionation (23, 59). Thus, the abiotic rates of S_x^{2-} formation and disproportionation, the former of which is dependent on the rate of H_2S produced by biological activity, and the kinetics of coarsening are likely to generate a distribution of soluble S^0 particle sizes during the incubation period that are available for use in metabolism. Consistent with this notion, the growth experiments with strain DS80 reported here and those reported previously for *A. sulfurireducens* (23) showed that the electron acceptor (i.e., nanoparticulate S^0) that supported growth exhibited an apparent size dependence, with higher rates of reduction and shorter generation times observed when S^0 was sequestered in dialysis membranes with larger pore sizes. These results suggest that a similar mechanism involving biological and abiological feedbacks likely supports S^0-dependent growth in strain DS80 (*Sulfolobales*) and *A. sulfurireducens* (*Desulfurococcales*) (22).

The mechanism of S^0 respiration with H_2 in *Acidianus* involves a short electron transfer chain comprising a membrane-bound S^0 reductase (SreABCD) and membrane-bound [NiFe]-hydrogenase complex (HynSL) (66). Homologs of these proteins are encoded in the genome of strain DS80 (Amenabar et al., submitted), suggesting that it likely uses the same mechanism to respire S^0. To our knowledge, there is no evidence for the involvement of extracellular enzymes in S^0 reduction in members of the *Acidianus* genus.

The requirement for direct access to S^0 differed depending on whether DS80 cells were using the mineral as an oxidant, as a reductant, or as both a reductant and an oxidant (disproportionation). Like DS80 cells grown via S^0 reduction, those grown via S^0 disproportionation (Fig. 4A, B, and C) did not require direct access to the mineral to use it in their energy metabolism, suggesting that the H_2S formed through this process functioned to solubilize S^0 through a mechanism like what is described above for S^0-reducing cells. However, unlike DS80 cells reducing or disproportionating S^0, cells that were oxidizing S^0 required direct access to the mineral. The requirement for direct contact to S^0 to oxidize it is consistent with microscopic observations of cultures of other S^0-oxidizing crenarchaeotes such as *Sulfolobus* spp., which were shown to be attached to S^0 crystals both in lab cultures and in samples collected from various hot-spring environments (67). The results of the dialysis membrane experiments with cultures oxidizing S^0, which show no growth or activity when S^0 is sequestered, also further substantiate the proposed mechanism for how cells access S^0 under reducing conditions, since the H_2S needed to initiate the series of abiotic reactions that solubilize S^0 was incapable of being produced (23).

The lack of detectable SO_4^{2-} in cultures of DS80 provided with H_2/S^0 (data not shown) and the stoichiometry of the products formed during growth with S^0/Fe(III) [to control for potential abiotic oxidation of H_2S by Fe(III) and to discount that cells were growing via disproportionation] suggest that the presence of H_2 or Fe(III) favors growth via reduction or oxidation of S^0, respectively, over disproportionation. This is likely a

Downloaded from http://aem.asm.org/ on May 31, 2018 by MONTANA STATE UNIV AT BOZEMAN

consequence of the energetic yields of these reactions, where the standard Gibbs free energy change ($\Delta G°$) at 80°C for the H_2/S^0 and S^0/Fe(III) redox couples are -47.57 kJ mol^{-1} and -298.76 kJ mol^{-1}, respectively, in comparison to the thermodynamically unfavorable $\Delta G°$ of 121.71 kJ mol^{-1} for the S^0 disproportionation condition ($\Delta G°$ calculations were performed as previously described [27]). Consistent with the thermodynamic constraints for the S^0 disproportionation growth condition, initial attempts to cultivate strain DS80 via disproportionation failed (data not shown). To produce and maintain favorable thermodynamics in bacterial cultures growing via S^0 disproportionation at circumneutral to alkaline pH, other researchers have added compounds to scavenge sulfide, such as Fe(III) minerals (31, 33–35). However, for reasons mentioned above, adding Fe(III) to cultures of DS80 designed to grow via the disproportionation condition would promote growth via S^0 oxidation and Fe(III) reduction (27). To overcome this limitation, we maximized the headspace-to-liquid volume ratio in our cultures (while still allowing for enough volume for sampling) to keep aqueous sulfide concentrations as low as possible. In doing so, we maintained favorable thermodynamics for the reaction over the course of a cultivation cycle (Fig. 4D) and were able to demonstrate this biological activity. This study reports a microbial strain that can reduce, oxidize, and disproportionate S^0.

The ΔG of the S^0 disproportionation reaction that sustained activity and cell production in cultures of DS80 ranged from -73.4 kJ mol^{-1} to -32.9 kJ mol^{-1} [-18.3 to -8.2 kJ (mol $e^-)^{-1}$ transferred, respectively] (Fig. 4D). This range of values is similar to those (-30 kJ mol^{-1}) calculated for several bacterial strains growing via S^0 disproportionation (68) but is lower than the estimated value of -92 kJ mol^{-1} for two neutrophilic bacterial cultures (34). Nonetheless, the ΔG for cultures of DS80 during the growth cycle is close to the minimum Gibbs energy yield of -20 kJ mol^{-1} suggested to be required to sustain microbial life (69), a value which is based on the energetics associated with formation of 1/3 of a mole of ATP from ADP and P_i. Growth of strain DS80 would be expected to be more favorable in a natural, open system where products (i.e., H_2S and SO_4^{2-}) could be potentially exsolved, flushed from the system, or consumed by another member of the community.

DS80 cells grew via reduction of iron (hydr)oxide minerals without direct access to the mineral surface (Fig. 5A and B), albeit with lower rates and slower generation times than when provided with access to the surface. The increased iron reduction rates and generation times in cultures provided with direct access to iron oxide minerals suggest that cells can either directly reduce solid-phase iron minerals or promote their dissolution, leading to greater availability of Fe(III) ions for reduction. Fe(III) ions or complexes would be able to diffuse across the dialysis membrane, allowing for iron reduction activity without direct access to the mineral, albeit at potentially lower rates due to diffusional constraints. Consistent with the hypothesis that cells are reducing soluble Fe(III) ions, growth assays indicated that the soluble form of iron that supports iron reduction does not exhibit a size distribution. Iron-bearing minerals are more soluble under acidic conditions, with the minimum solubilities typically observed in solutions with neutral to alkaline pH (70). We suggest that under acidic conditions, such as those present in the environments where *Acidianus* strain DS80 and related strains have been detected, microorganisms are poised to reduce soluble Fe(III) ions leached from precipitated iron minerals through a proton-promoted dissolution mechanism (70). Consistent with the notion of cells reducing a solubilized form of Fe and not the bulk mineral, microscopy indicates that DS80 cells are not obligately associated with ferrihydrite when they are given access to the mineral (27).

Observations indicating that DS80 cells are likely reducing a soluble form of Fe(III) prompted additional experimentation aimed at characterizing the effect of Fe(III) mineral solubility on the rate of Fe(III) reduction. Cells of strain DS80 utilized a variety of Fe(III) sources as electron acceptors, including ferric sulfate, ferrihydrite, goethite, and hematite (see Fig. S5 in the supplemental material). Rates of Fe(III) reduction when autotrophically grown cells were supplied with ferric sulfate, ferrihydrite, goethite, and hematite as an electron acceptor and S^0 as an electron donor were 2,532 $\pm$ 450 nmol

Downloaded from http://aem.asm.org/ on May 31, 2018 by MONTANA STATE UNIV AT BOZEMAN

h^{-1}, 238 ± 1 nmol h^{-1}, 93 ± 4 nmol h^{-1}, and 39 ± 2 nmol h^{-1}, respectively. These rates of Fe(III) reduction were broadly consistent with the equilibrium solubilities of the different iron sources tested, i.e., ferric sulfate > ferrihydrite (K_s = 3.55) > goethite (K_s = 0.36) > hematite (K_s = −0.53) (70), with higher rates of reduction with poorly crystalline ferrihydrite than with crystalline hematite. With the data collected, it is difficult to deconvolute whether this decrease in Fe reduction rate with increased mineral crystallinity is due to an increased ease by which electrons can be deposited into poorly crystalline mineral lattices, as has been shown for a *Shewanella alga* strain (71), or whether this is due to increased reduction of soluble Fe(III) ions due to differences in mineral solubility. Nonetheless, the ability to reduce both soluble and insoluble Fe(III) is advantageous in acidic hot-spring systems, since both Fe(III) ions (see Fig. S1C in the supplemental material) (15) and a variety of Fe oxides are often available in these systems (41, 42, 72).

Strain DS80 was shown to grow via oxidation of the arsenic sulfide mineral α-As_4S_4 without direct access to the mineral surface (Fig. 6A, B, and C) when Fe(III) served as an electron acceptor. This suggests the possibility of an abiotic oxidative dissolution mechanism catalyzed by Fe(III) ions in providing soluble As to support the growth of DS80. Abiotic oxidation of α-As_4S_4 in the presence of O_2 has been shown to yield As(III) and As(V), with As(III) as the dominant species (73). Like O_2, Fe(III) is also known as a strong oxidant under acidic conditions and has been shown to increase the rates of oxidation and dissolution of the arsenic sulfide mineral arsenopyrite (74). However, the influence of Fe(III) ions on the oxidative dissolution of other As-bearing sulfides such as α-As_4S_4 has not been investigated in detail (74). Zhang et al. (75) showed that the leaching rate of As from α-As_4S_4 increases in cultures of the acidophilic bacterium *Acidithiobacillus ferrooxidans* grown with Fe(II) as an electron donor compared to cultures not provided with Fe(II). This observation was attributed to the formation of Fe(III) during growth of *A. ferrooxidans*, since abiotic experiments indicated that Fe(II) did not have any effect on the rate of oxidation of α-As_4S_4. The oxidative dissolution of α-As_4S_4 by Fe(III) has been reported to yield both As(III) and S^0 as products (75), consistent with our observation that neither SO_4^{2-} nor H_2S was formed during growth with α-As_4S_4 as the sole electron donor. The observation that cells of strain DS80 were not able to oxidize α-As_4S_4 when O_2 was provided as an electron acceptor but could oxidize As(III) when O_2 was provided as electron acceptor suggests that the rate of O_2-promoted oxidative dissolution of α-As_4S_4 to yield soluble components capable of serving as electron donor was not high enough to support growth. This is consistent with the observation that Fe(III) ions are more efficient in extracting electrons from metal sulfide lattices than O_2 (76, 77). In addition to Fe(III) ions, α-As_4S_4 could also be solubilized by protons, resulting in the leaching of As from the mineral and the formation of S^0 via intermediary polysulfides (78). However, this second mechanism of proton-promoted α-As_4S_4 dissolution is discounted, since cells were not able to grow with O_2 as an electron acceptor and since polysulfides are unstable in aqueous solutions with pHs of <6.0 (79–81).

Conclusions. The evidence presented here indicates that strain DS80 can use a wide spectrum of redox-active minerals that are commonly identified in acidic hot springs to support cell growth and metabolism. These observations may help to explain the apparent widespread distribution of this and related strains across broad temperature, pH, and mineralogical gradients in hot springs. Other *Acidianus* strains may be equally flexible in their mineral-dependent metabolism, which may help to explain the widespread distribution of this genus in geochemically diverse hydrothermal environments in YNP and in other hydrothermal fields, including both terrestrial and marine thermal sites (45, 47, 82–84).

The demonstrated ability of DS80 to grow via transformation of minerals suggests that it likely influences the chemical composition of its hydrothermal environment. As an example, there is no direct evidence that Fe(III) reduction is occurring in the iron (hydro)oxide depositional zone in Dragon Spring; however, the limited accumulation of

Downloaded from http://aem.asm.org/ on May 31, 2018 by MONTANA STATE UNIV AT BOZEMAN

iron (hydr)oxide (<1-cm depth in many regions) suggests that Fe(III) reduction or proton-promoted dissolution must be an important component of the Fe cycle in these microbial mats (21). The ability of strain DS80 to reduce iron minerals with either H_2 or S^0 under conditions mimicking those of the spring environment may explain the limited accumulation of iron (hydr)oxide observed in Dragon Spring. The same could be true for S^0, where we have observed rain events where the entirety of the S^0 mats present in Dragon Spring were flushed out of the system, only to reappear within the next several days. This suggests that the rate of S^0 precipitation, which must be high, is likely to be balanced by the rate of utilization by strains such as DS80 or other S^0-reducing/disproportionating populations identified in this spring (22) or by natural flushing of the flocculent mineral.

Strain DS80 was shown to reduce, oxidize, and disproportionate S^0, indicating that the strain is adapted to grow in sulfur-rich hot-spring habitats where the availabilities of electron donors (e.g., H_2) and electron acceptors (e.g., ferric iron) are likely to vary, both spatially and temporally (85). Growth of strain DS80 under disproportionating conditions was observed under conditions approaching thermodynamic equilibrium [−18.3 to −8.2 kJ (mol e^-)$^{-1}$ transferred], and this value was strongly dependent on the concentration of dissolved sulfide. This underscores the importance of sulfide-scavenging mechanisms, either biological or abiological, in natural environments in maintaining the thermodynamic favorability of this process. Sulfide exsolving from the local environment (the pKa of H_2S is 6.4 at 80°C [5]) is also likely to be an important process allowing for disproportionation to remain thermodynamically favorable under natural conditions. This study reports the occurrence of S^0 disproportionation in an acidophile and in an archaeon, thereby broadening the taxonomic and ecological space for where this process is of putative importance. In addition, this study reports a themoacidophilic microorganism capable of oxidizing α-As_4S_4, albeit indirectly, to support its growth.

Different minerals and different modes of metabolism imparted different requirements for surface access during growth. Cells reducing iron minerals did not require access to those minerals to support growth, presumably due to leaching of Fe(III) ions by the acidity of the growth medium, although growth and iron reduction activities were higher when direct access to the mineral was provided. Cells oxidizing S^0 required direct access to the mineral, whereas those reducing or disproportionating S^0 did not. A series of abiotic and biotic reaction feedbacks involving the biological production of H_2S, the formation of unstable S_x^{2-}, and the coarsening of nanoparticulate S^0 are implicated in explaining these differences. Importantly, the interplay between the biological and abiological kinetics of reactions involving Fe, S, and As compounds likely influences their bioavailability for use in microbial metabolism; more work is needed to identify the rate-limiting step in these proposed mechanisms and to determine if and how this constrains the activity of microbial populations. We suggest that a similar interplay of biotic- and abiotic-catalyzed processes is taking place in hot-spring environments and that together they increase the availability of minerals capable of supporting microbial metabolism and growth.

MATERIALS AND METHODS

DNA extraction and PCR amplification of the sulfur oxygenase reductase (*sor*) gene. Sediments from 73 thermal features in YNP were collected aseptically as previously described (86). Sampling sites were chosen to include a wide range of temperature and pH combinations available in the thermal features of YNP as well as to sample geographically distinct areas of the park. The pH and temperature of each thermal feature were measured on-site with a YSI pH100CC-01 pH meter and a YSI EC300 conductivity meter (YSI, Inc., USA), respectively. Genomic DNA was extracted from approximately 100 mg of sediment using the FastDNA spin kit for soils (MP Biomedicals, Santa Ana, CA). Genomic DNAs from five isolates (see below and the supplemental material for descriptions) were also extracted using this kit. The concentration of DNA in the extract was determined using a Qubit 2.0 fluorimeter (Invitrogen, Carlsbad, CA, USA) and a Qubit double-stranded DNA (dsDNA) HS assay kit (Molecular Probes, Eugene, OR, USA).

DNA extracts were subjected to PCR amplification of archaeal and bacterial 16S rRNA genes. PCR amplification of 16S rRNA genes was performed according to previously described protocols (87, 88) using archaeal primers 344F (5′-ACGGGGYGCAGCAGGCGCGA-3′) and 915R (5′-GTGCTCCCCCGCCAATTC

Downloaded from http://aem.asm.org/ on May 31, 2018 by MONTANA STATE UNIV AT BOZEMAN

CT-3′) and bacterial primers 1100F (5′-YAACGAGCGCAACCC-3′) and 1492R (5′-GGTTACCTTGTTACGACT T-3′). An annealing temperature of 55°C or 61°C was used for bacterial or archaeal primers, respectively. Bacterial and/or archaeal 16S rRNA genes were obtained from all hot-spring sediment/mat DNA extracts. Bacterial 16S rRNA gene amplicons were not detected in any of the DNA extracts from isolated cultivars. Archaeal 16S rRNA gene amplicons from each isolate were purified, cloned, sequenced, assembled, and analyzed using previously published methods (88).

Purified DNA extracts were also subjected to PCR amplification of the *sor* gene. Primers sorF (5′-GGACCTTGGGAGCCAATTTA-3′) and sorR (5′-CTCCAGAATGTTCCTTCCATCA-3′) were designed to target positions 10 to 588 in the *sor* gene from *Acidianus* strain DS80 (IMG gene ID 2690452492, genome ID 2690315630) as well as other *sor* homologs from *Acidianus* spp. available in the NCBI database. These primers were specifically designed not to amplify the *sor* fragment from closely related *Sulfolobales* strains (e.g., *Sulfolobus tokodaii* [BA000023]) or other sulfur oxidizers carrying the *sor* gene, such as *Picrophilus torridus* (AE017261), *Ferroplasma acidiphilum* (CP015363), *Ferroplasma*, *acidarmanus* (CP004145), *Sulfobacillus acidophilus* (CP003179), *Acidithiobacillus thiooxidans* (KJ483962), *Acidithiobacillus caldus* (KJ958902), *Acidithiobacillus ferrivorans* (CP002985), *Halothiobacillus neapolitanus* (CP001801), *Acidihalobacter ferrooxidans* (CP019434), *Thioalkalivibrio nitratireducens* (CP003989), *Thioalkalivibrio paradoxus* (CP007029), and *Aquifex aeolicus* (AE000657). PCR amplification of *sor* was optimized using genomic DNA from *Acidianus* sp. strain DS80 as a positive control and genomic DNA from *S. tokodaii* (kindly provided by Mark Young) as a negative control. PCR cycling conditions included an initial 4-min denaturation step (94°C) followed by 30 rounds of denaturation (94°C, 1 min), annealing (50°C, 1 min), and extension (72°C, 1 min), with a final 15-min extension step at 72°C. PCR mixtures included ~0.5 ng of DNA, 1.5 mM $MgCl_2$ (Invitrogen), 200 μM each deoxynucleoside triphosphate (Sigma-Aldrich, USA), 0.5 μM each forward and reverse primer, 0.4 μg μl^{-1} molecular-grade bovine serum albumin (Roche, USA), and 0.25 U *Taq* DNA polymerase (Invitrogen) in 1× PCR buffer (Invitrogen) (50-μl final volume). PCR amplification was verified by electrophoresis in a 1.5% agarose gel.

Culture conditions. *Acidianus* strain DS80, previously isolated from Dragon Spring (YNP thermal inventory ID NHSP042), was cultivated in anoxic base salts mineral medium containing NH_4Cl (0.33 g liter^{-1}), KCl (0.33 g liter^{-1}), $CaCl_2 \cdot 2H_2O$ (0.33 g liter^{-1}), $MgCl_2 \cdot 6H_2O$ (0.33 g liter^{-1}), and KH_2PO_4 (0.33 g liter^{-1}) as previously described (27). The pH of the medium was adjusted to 3.0 with concentrated hydrochloric acid. Briefly, 55 ml of medium was dispensed into 160-ml serum bottles and was subjected to autoclave sterilization. For growth via S^0 disproportionation, 18 ml of medium was used instead of 55 ml to increase the headspace/liquid volume ratio. This allowed for greater partitioning of H_2S into the gas phase (the pKa of H_2S_g/HS^- is ~6.4 at 80°C [5]), thereby maintaining a more favorable environment (thermodynamically) for this redox reaction during the incubation period, as described in more detail in Discussion. Following autoclave sterilization and while still hot (~90°C), filter-sterilized (0.22-μm filter) Wolfe's vitamins (1 ml liter^{-1} final concentration) and filter sterilized (0.22-μm filter) SL-10 trace metals (1 ml liter^{-1} final concentration) were added. S^0 (sterilized by baking dry at 100°C for 24 h) was added at a final concentration of 5 g liter^{-1}. Commercially obtained α-As_4S_4 (95%; Sigma-Aldrich, USA) was also sterilized by baking dry at 100°C for 24 h and was added at a final concentration of 0.36 g liter^{-1}. $Fe_2(SO_4)_3 \cdot H_2O$ (sterilized by 0.22-μm filtration) was added at a final concentration of 3.7 g liter^{-1}, while ferrihydrite (prepared aseptically using sterilized reagents according to previously described procedures [89]) was added at a final concentration of 0.25 g liter^{-1}. Briefly, ferrihydrite was formed by neutralizing a filter-sterilized (0.22-μm filter) 0.4 M solution of $FeCl_3$ to a pH of 7.0 with filter-sterilized (0.22-μm filter) NaOH, followed by washing with filter-sterilized (0.22-μm filter) deionized water. The suspension of synthetically produced ferrihydrite was deoxygenated by stirring under sterile N_2 passed over heated (210°C) and hydrogen (H_2)-reduced copper shavings and repeated flushing of the headspace in a sealed serum bottle.

Following addition of nutrient amendments, the bottles and their contents were deoxygenated by purging with O_2-free, sterile nitrogen (N_2), as described above. The serum bottles were sealed with butyl rubber stoppers and heated to 80°C prior to the replacement of the headspace. A headspace gas mixture of N_2-CO_2 (80%:20%) was used when S^0 was supplied as the electron donor and Fe(III) as the electron acceptor, when S^0 was supplied as the electron donor and acceptor (disproportionation), and when α-As_4S_4 was supplied as the electron donor and Fe(III) as the electron acceptor. A headspace gas mixture of H_2-CO_2 (80%:20%) was used when H_2 served as the electron donor and S^0 or Fe(III) (soluble and mineral) as the electron acceptor. All cultures were grown autotrophically in medium with a pH of 3.0 and were incubated at 80°C. Unless otherwise stated, all growth experiments were performed in triplicate, and a single uninoculated control was included for use in monitoring abiotic chemical reactions.

Mineral surface requirements. The requirement for physical contact with minerals when they serve as electron donor, electron acceptor, or both electron donor and acceptor (disproportionation conditions) was evaluated by sequestering minerals in dialysis tubing with various pore size diameters, as previously described (23). Five different growth conditions were examined: (i) H_2 as electron donor and S^0 as electron acceptor, (ii) S^0 as electron donor and ferric sulfate as electron acceptor, (iii) S^0 as electron donor and acceptor (disproportionation), (iv) H_2 as electron donor and ferrihydrite as electron acceptor, and (v) α-As_4S_4 as electron donor and ferric sulfate as electron acceptor. S^0 was sequestered in dialysis tubing under the first three conditions, while ferrihydrite and α-As_4S_4 were sequestered in dialysis tubing under the last two conditions, respectively. S^0, ferrihydrite, or α-As_4S_4 was added to dialysis membranes (Spectrum Laboratories, Gardena, CA) with pore sizes of 6 to 8 kDa or 12 to 14 kDa, followed by closure with dialysis clips. Prior to use, all dialysis membranes were incubated at 80°C in nanopure (18.2 MΩ cm^{-1}) deionized water for 4 h to remove preservatives, and this process was repeated a total of 3 times, with replacement of the deionized water each of the times. Experiments where direct contact between

Downloaded from http://aem.asm.org/ on May 31, 2018 by MONTANA STATE UNIV AT BOZEMAN

cells and minerals was allowed (when S^0, ferrihydrite, or α-As_4S_4 was not sequestered) were performed in the presence of dialysis membranes (12 to 14 kDa) to account for the potential interactions between cells, membranes, and/or minerals.

Evaluation of growth and activity. The growth and activity of strain DS80 with different electron donors and acceptors were quantified in terms of cell density and production of total sulfide (S^{2-}; proxy for S^0 reduction or disproportionation), production of sulfate (SO_4^{2-}; proxy for S^0 oxidation or disproportionation), or production of ferrous iron [Fe(II); proxy for Fe(III) reduction] using methods previously described (27). Dissolved sulfide concentrations were determined with the methylene blue reduction method (90). Total sulfide production (dissolved and gaseous) was calculated using standard gas-phase equilibrium calculations as described previously (22). The concentration of ferrous iron was determined using the Ferrozine method (91), and the concentration of sulfate was determined after precipitation with barium chloride, as previously described (92). The concentration of As(V) [proxy for As(III) oxidation] was determined by colorimetry after its complexation with molybdate, as previously described (93).

SUPPLEMENTAL MATERIAL

Supplemental material for this article may be found at https://doi.org/10.1128/AEM.00334-18.

SUPPLEMENTAL FILE 1, PDF file, 0.6 MB.

ACKNOWLEDGMENTS

This work was supported by the NASA Exobiology and Evolutionary Biology program (NNX13AI11G to E.S.B.). The NASA Astrobiology Institute is supported by grant number NNA15BB02A to E.S.B. M.J.A. acknowledges support from the CONICYT Becas-Chile Scholarship program.

We declare that we have no conflict of interest.

REFERENCES

1. Boyd ES, Hamilton TL, Spear JR, Lavin M, Peters JW. 2010. [FeFe]-hydrogenase in Yellowstone National Park: evidence for dispersal limitation and phylogenetic niche conservatism. ISME J 4:1485–1495. https://doi.org/10.1038/ismej.2010.76.
2. Cox A, Shock EL, Havig JR. 2011. The transition to microbial photosynthesis in hot spring ecosystems. Chem Geol 280:344–351. https://doi.org/10.1016/j.chemgeo.2010.11.022.
3. Boyd ES, Fecteau KM, Havig JR, Shock EL, Peters JW. 2012. Modeling the habitat range of phototrophs in Yellowstone National Park: toward the development of a comprehensive fitness landscape. Front Microbiol 3:221. https://doi.org/10.3389/fmicb.2012.00221.
4. Hamilton TL, Vogl K, Bryant DA, Boyd ES, Peters JW. 2012. Environmental constraints defining the distribution, composition, and evolution of chlorophototrophs in thermal features of Yellowstone National Park. Geobiology 10:236–249. https://doi.org/10.1111/j.1472-4669.2011.00296.x.
5. Amend JP, Shock EL. 2001. Energetics of overall metabolic reactions of thermophilic and hyperthermophilic Archaea and Bacteria. FEMS Microbiol Rev 25:175–243. https://doi.org/10.1111/j.1574-6976.2001.tb00576.x.
6. Urschel MR, Kubo MD, Hoehler TM, Peters JW, Boyd ES. 2015. Carbon source preference in chemosynthetic hot spring communities. Appl Environ Microbiol 81:3834–3847. https://doi.org/10.1128/AEM.00511-15.
7. Spear JR, Walker JJ, McCollom TM, Pace NR. 2005. Hydrogen and bioenergetics in the Yellowstone geothermal ecosystem. Proc Natl Acad Sci U S A 102:2555–2560. https://doi.org/10.1073/pnas.0409574102.
8. Nordstrom DK, Ball JW, McCleskey RB. 2005. Ground water to surface water: chemistry of thermal outflows in Yellowstone National Park, p 73–94. *In* Inskeep WP, McDermott TR (ed), Geothermal biology and geochemistry in Yellowstone National Park. Montana State University Publications, Bozeman, MT.
9. Fournier RO. 1989. Geochemistry and dynamics of the Yellowstone-National-Park hydrothermal system. Annu Rev Earth Planet Sci 17:13–53. https://doi.org/10.1146/annurev.ea.17.050189.000305.
10. Truesdell AH, Fournier RO. 1976. Conditions in the deeper parts of the hot spring systems of Yellowstone National Park, Wyoming. Open-file report 76-428. U.S. Geological Survey, Reston, VA.
11. White DE, Muffler LJP, Truesdell AH. 1971. Vapor-dominated hydrothermal systems compared with hot-water systems. Econ Geol 66:75–97. https://doi.org/10.2113/gsecongeo.66.1.75.
12. Nordstrom DK, McCleskey RB, Ball JW. 2009. Sulfur geochemistry of hydrothermal waters in Yellowstone National Park. IV. Acid-sulfate waters. Appl Geochem 24:191–207. https://doi.org/10.1016/j.apgeochem.2008.11.019.
13. Colman DR, Poudel S, Hamilton TL, Havig JR, Selensky MJ, Shock EL, Boyd ES. 2018. Geobiological feedbacks and the evolution of thermoacidophiles. ISME J 12:225–236. https://doi.org/10.1038/ismej.2017.162.
14. White DE, Hutchinson RA, Keith TE. 1988. Geology and remarkable thermal activity of Norris Geyser Basin, Yellowstone National Park, Wyoming. Professional paper 1456. US Geolological Survey, Reston, VA.
15. Ball JW, McMleskey RB, Nordstrom DK. 2010. Water-chemistry data for selected springs, geysers, and streams in Yellowstone National Park, Wyoming, 2006-2008. Open-file report 2010-1192. U.S. Geological Survey, Reston, VA.
16. Colman DR, Feyhl-Buska J, Robinson KJ, Fecteau KM, Xu H, Shock EL, Boyd ES. 2016. Ecological differentiation in planktonic and sediment-associated chemotrophic microbial populations in Yellowstone hot springs. FEMS Microbiol Ecol 92:fiw137. https://doi.org/10.1093/femsec/fiw137.
17. Amenabar MJ, Urschel MR, Boyd ES. 2015. Metabolic and taxonomic diversification in continental magmatic hydrothermal systems, p 57–96. *In* Bakermans C (ed), Microbial evolution under extreme conditions. De Gruyter, Berlin, Germany.
18. Inskeep WP, Rusch DB, Jay ZJ, Herrgard MJ, Kozubal MA, Richardson TH, Macur RE, Hamamura N, Jennings RD, Fouke BW, Reysenbach AL, Roberto F, Young M, Schwartz A, Boyd ES, Badger JH, Mathur EJ, Ortmann AC, Bateson M, Geesey G, Frazier M. 2010. Metagenomes from high-temperature chemotrophic systems reveal geochemical controls on microbial community structure and function. PLoS One 5:e9773. https://doi.org/10.1371/journal.pone.0009773.
19. Alsop EB, Boyd ES, Raymond J. 2014. Merging metagenomics and geochemistry reveals environmental controls on biological diversity and evolution. BMC Ecol 14:16. https://doi.org/10.1186/1472-6785-14-16.
20. Inskeep WP, Jay ZJ, Tringe SG, Herrgard MJ, Rusch DB, Co YMPS. 2013. The YNP metagenome project: environmental parameters responsible for microbial distribution in the Yellowstone geothermal ecosystem. Front Microbiol 4:67. https://doi.org/10.3389/fmicb.2013.00067.
21. Inskeep W, McDermott T. 2005. Geomicrobiology of acid-sulfate-chloride springs in Yellowstone National Park. p 143–162. *In* Inskeep WP, McDermott TR (ed), Geothermal biology and geochemistry in Yellowstone National Park. Montana State University Publications, Bozeman, MT.
22. Boyd ES, Jackson RA, Encarnacion G, Zahn JA, Beard T, Leavitt WD, Pi Y,

Downloaded from http://aem.asm.org/ on May 31, 2018 by MONTANA STATE UNIV AT BOZEMAN

Zhang CL, Pearson A, Geesey GG. 2007. Isolation, characterization, and ecology of sulfur-respiring crenarchaea inhabiting acid-sulfate-chloride-containing geothermal springs in Yellowstone National Park. Appl Environ Microbiol 73:6669–6677. https://doi.org/10.1128/AEM.01321-07.
23. Boyd ES, Druschel GK. 2013. Involvement of intermediate sulfur species in biological reduction of elemental sulfur under acidic, hydrothermal conditions. Appl Environ Microbiol 79:2061–2068. https://doi.org/10.1128/AEM.03160-12.
24. Xu Y, Schoonen MAA, Nordstrom DK, Cunningham KM, Ball JW. 1998. Sulfur geochemistry of hydrothermal waters in Yellowstone National Park. I. The origin of thiosulfate in hot spring waters. Geochim Cosmochim Acta 62:3729–3743. https://doi.org/10.1016/S0016-7037(98)00269-5.
25. Langner HW, Jackson CR, Mcdermott TR, Inskeep WP. 2001. Rapid oxidation of arsenite in a hot spring ecosystem, Yellowstone National Park. Environ Sci Technol 35:3302–3309. https://doi.org/10.1021/es0105562.
26. Friedrich CG, Rother D, Bardischewsky F, Quentmeier A, Fischer J. 2001. Oxidation of reduced inorganic sulfur compounds by bacteria: Emergence of a common mechanism? Appl Environ Microbiol 67:2873–2882. https://doi.org/10.1128/AEM.67.7.2873-2882.2001.
27. Amenabar MJ, Shock EL, Roden EE, Peters JW, Boyd ES. 2017. Microbial substrate preference dictated by energy demand rather than supply. Nat Geosci 10:577–581. https://doi.org/10.1038/ngeo2978.
28. Huber H, Prangishvili D. 2006. Sulfolobales, p 23–51. *In* Dworkin M, Falkow S, Rosenberg E, Schleifer KH, Stackebrandt E (ed), The prokaryotes: a handbook on the biology of bacteria, 3rd ed, vol 3. Springer, New York, NY.
29. Boyd ES, Leavitt WD, Geesey GG. 2009. CO2 uptake and fixation by a thermoacidophilic microbial community attached to precipitated sulfur in a geothermal spring. Appl Environ Microbiol 75:4289–4296. https://doi.org/10.1128/AEM.02751-08.
30. Muyzer G, Stams AJM. 2008. The ecology and biotechnology of sulphate-reducing bacteria. Nat Rev Microbiol 6:441–454. https://doi.org/10.1038/nrmicro1892.
31. Janssen PH, Schuhmann A, Bak F, Liesack W. 1996. Disproportionation of inorganic sulfur compounds by the sulfate-reducing bacterium *Desulfocapsa thiozymogenes* gen nov, sp nov. Arch Microbiol 166:184–192. https://doi.org/10.1007/s002030050374.
32. Lovley DR, Phillips EJP. 1994. Novel processes for anaerobic sulfate production from elemental sulfur by sulfate-reducing bacteria. Appl Environ Microbiol 60:2394–2399.
33. Slobodkin AI, Reysenbach AL, Slobodkina GB, Baslerov RV, Kostrikina NA, Wagner ID, Bonch-Osmolovskaya EA. 2012. *Thermosulfurimonas dismutans* gen nov, sp nov, an extremely thermophilic sulfur-disproportionating bacterium from a deep-sea hydrothermal vent. Int J Syst Evol Microbiol 62:2565–2571. https://doi.org/10.1099/ijs.0.034397-0.
34. Thamdrup B, Finster K, Hansen JW, Bak F. 1993. Bacterial disproportionation of elemental sulfur coupled to chemical-reduction of iron or manganese. Appl Environ Microbiol 59:101–108.
35. Finster K, Liesack W, Thamdrup B. 1998. Elemental sulfur and thiosulfate disproportionation by *Desulfocapsa sulfoexigens* sp. nov., a new anaerobic bacterium isolated from marine surface sediment. Appl Environ Microbiol 64:119–125.
36. Lovley DR, Holmes DE, Nevin KP. 2004. Dissimilatory Fe(III) and Mn(IV) reduction. Adv Microb Physiol 49:219–286. https://doi.org/10.1016/S0065-2911(04)49005-5.
37. Fortney NW, He S, Converse BJ, Beard BL, Johnson CM, Boyd ES, Roden EE. 2016. Microbial Fe(III) oxide reduction potential in Chocolate Pots hot spring, Yellowstone National Park. Geobiology 14:255–275. https://doi.org/10.1111/gbi.12173.
38. Kashefi K, Shelobolina ES, Elliott WC, Lovley DR. 2008. Growth of thermophilic and hyperthermophilic Fe(III)-reducing microorganisms on a ferruginous smectite as the sole electron acceptor. Appl Environ Microbiol 74:251–258. https://doi.org/10.1128/AEM.01580-07.
39. Slobodkin AI. 2005. Thermophilic microbial metal reduction. Microbiology 74:501–514. https://doi.org/10.1007/s11021-005-0096-6.
40. Slobodkina GB, Panteleeva AN, Sokolova TG, Bonch-Osmolovskaya EA, Slobodkin AI. 2012. *Carboxydocella manganica* sp nov, a thermophilic, dissimilatory Mn(IV)- and Fe(III)-reducing bacterium from a Kamchatka hot spring. Int J Syst Evol Microbiol 62:890–894. https://doi.org/10.1099/ijs.0.027623-0.
41. Kozubal M, Macur RE, Korf S, Taylor WP, Ackerman GG, Nagy A, Inskeep WP. 2008. Isolation and distribution of a novel iron-oxidizing crenarchaeon from acidic geothermal springs in Yellowstone National Park. Appl Environ Microbiol 74:942–949. https://doi.org/10.1128/AEM.01200-07.
42. Inskeep WP, Macur RE, Harrison G, Bostick BC, Fendorf S. 2004. Biomineralization of As(V)-hydrous ferric oxyhydroxide in microbial mats of an acid-sulfate-chloride geothermal spring, Yellowstone National Park. Geochim Cosmochim Acta 68:3141–3155. https://doi.org/10.1016/j.gca.2003.09.020.
43. Johnson DB, Kanao T, Hedrich S. 2012. Redox transformations of iron at extremely low pH: fundamental and applied aspects. Front Microbiol 3:96. https://doi.org/10.3389/fmicb.2012.00096.
44. Beam JP, Bernstein HC, Jay ZJ, Kozubal MA, deM Jennings R, Tringe SG, Inskeep WP. 2016. Assembly and succession of iron oxide microbial mat communities in acidic geothermal springs. Front Microbiol 7:25. https://doi.org/10.3389/fmicb.2016.00025.
45. Yoshida N, Nakasato M, Ohmura N, Ando A, Saiki H, Ishii M, Igarashi Y. 2006. *Acidianus manzaensis* sp nov, a novel thermoacidophilic archaeon growing autotrophically by the oxidation of H_2 with the reduction of Fe^{3+}. Curr Microbiol 53:406–411. https://doi.org/10.1007/s00284-006-0151-1.
46. Kozubal MA, Macur RE, Jay ZJ, Beam JP, Malfatti SA, Tringe SG, Kocar BD, Borch T, Inskeep WP. 2012. Microbial iron cycling in acidic geothermal springs of Yellowstone National Park: integrating molecular surveys, geochennical processes, and isolation of novel Fe-active microorganisms. Front Microbiol 3:109. https://doi.org/10.3389/fmicb.2012.00109.
47. Giaveno MA, Urbieta MS, Ulloa JR, Toril EG, Donati ER. 2013. Physiologic versatility and growth flexibility as the main characteristics of a novel thermoacidophilic *Acidianus* strain isolated from Copahue geothermal area in Argentina. Microb Ecol 65:336–346. https://doi.org/10.1007/s00248-012-0129-4.
48. Webster JG, Nordstrom DK. 2003. Geothermal arsenic, p 101–125. *In* Welch AH, Stollenwerk KG (ed), Arsenic in ground water. Springer, Boston, MA.
49. Weed WH, Pirsson L. 1891. Occurrence of sulphur, orpiment, and realgar in the Yellowstone National Park. Am J Sci 42:401–405.
50. Masscheleyn PH, Delaune RD, Patrick WH, Jr. 1991. Effect of redox potential and pH on arsenic speciation and solubility in a contaminated soil. Environ Sci Technol 25:1414–1419. https://doi.org/10.1021/es00020a008.
51. Lewis AE. 2010. Review of metal sulphide precipitation. Hydrometallurgy 104:222–234. https://doi.org/10.1016/j.hydromet.2010.06.010.
52. Macur RE, Jay ZJ, Taylor W, Kozubal MA, Kocar BD, Inskeep WP. 2013. Microbial community structure and sulfur biogeochemistry in mildly-acidic sulfidic geothermal springs in Yellowstone National Park. Geobiology 11:86–99. https://doi.org/10.1111/gbi.12015.
53. Donahoe-Christiansen J, D'Imperio S, Jackson CR, Inskeep WP, McDermott TR. 2004. Arsenite-oxidizing *Hydrogenobaculum* strain isolated from an acid-sulfate-chloride geothermal spring in Yellowstone National Park. Appl Environ Microbiol 70:1865–1868. https://doi.org/10.1128/AEM.70.3.1865-1868.2004.
54. Oremland RS, Stolz JF. 2003. The ecology of arsenic. Science 300:939–944. https://doi.org/10.1126/science.1081903.
55. Jackson CR, Langner HW, Donahoe-Christiansen J, Inskeep WP, McDermott TR. 2001. Molecular analysis of microbial community structure in an arsenite-oxidizing acidic thermal spring. Environ Microbiol 3:532–542. https://doi.org/10.1046/j.1462-2920.2001.00221.x.
56. Huber H, Stetter KO. 2015. *Acidianus*, p 1–5. *In* Whitman WB, Rainey F, Kampfer P, Trujillo M, Chun J, DeVos P, Hedlund B, Dedysh S (ed), Bergey's manual of systematics of archaea and bacteria. Wiley Online Library. John Wiley & Sons, New York, NY.
57. Hochstein RA, Amenabar MJ, Munson-McGee JH, Boyd ES, Young MJ. 2016. *Acidianus* yailed spindle virus: a new archaeal large tailed spindle virus discovered by culture-independent methods. J Virol 90:3458–3468. https://doi.org/10.1128/JVI.03098-15.
58. You XY, Liu C, Wang SY, Jiang CY, Shah SA, Prangishvili D, She QX, Liu SJ, Garrett RA. 2011. Genomic analysis of *Acidianus hospitalis* W1 a host for studying crenarchaeal virus and plasmid life cycles. Extremophiles 15:487–497. https://doi.org/10.1007/s00792-011-0379-y.
59. Garcia AA, Druschel GK. 2014. Elemental sulfur coarsening kinetics. Geochem Trans 15:11. https://doi.org/10.1186/s12932-014-0011-z.
60. Reysenbach AL, Liu YT, Banta AB, Beveridge TJ, Kirshtein JD, Schouten S, Tivey MK, Von Damm KL, Voytek MA. 2006. A ubiquitous thermoacidophilic archaeon from deep-sea hydrothermal vents. Nature 442:444–447. https://doi.org/10.1038/nature04921.

Downloaded from http://aem.asm.org/ on May 31, 2018 by MONTANA STATE UNIV AT BOZEMAN

61. Urbieta MS, Rascovan N, Castro C, Revale S, Giaveno MA, Vazquez M, Donati ER. 2014. Draft genome sequence of the novel thermoacidophilic archaeon *Acidianus copahuensis* strain ALE1, isolated from the Copahue volcanic area in Neuquén, Argentina. Genome Announc 2:e00259-14. https://doi.org/10.1128/genomeA.00259-14.
62. Shi L, Squier TC, Zachara JM, Fredrickson JK. 2007. Respiration of metal (hydr)oxides by *Shewanella* and *Geobacter*: a key role for multihaem c-type cytochromes. Mol Microbiol 65:12–20. https://doi.org/10.1111/j.1365-2958.2007.05783.x.
63. Nealson KH, Scott J. 2006. Ecophysiology of the genus *Shewanella*, p 1133–1151. *In* Dworkin M, Falkow S, Rosenberg E, Schleifer KH, Stackebrandt E (ed), The prokaryotes: a handbook on the biology of bacteria, 3rd ed, vol 7. Springer, New York, NY.
64. Fredrickson JK, Romine MF, Beliaev AS, Auchtung JM, Driscoll ME, Gardner TS, Nealson KH, Osterman AL, Pinchuk G, Reed JL. 2008. Towards environmental systems biology of *Shewanella*. Nat Rev Microbiol 6:592. https://doi.org/10.1038/nrmicro1947.
65. Shi LA, Richardson DJ, Wang ZM, Kerisit SN, Rosso KM, Zachara JM, Fredrickson JK. 2009. The roles of outer membrane cytochromes of *Shewanella* and *Geobacter* in extracellular electron transfer. Environ Microbiol Rep 1:220–227. https://doi.org/10.1111/j.1758-2229.2009.00035.x.
66. Laska S, Lottspeich F, Kletzin A. 2003. Membrane-bound hydrogenase and sulfur reductase of the hyperthermophilic and acidophilic archaeon *Acidianus ambivalens*. Microbiology 149:2357–2371. https://doi.org/10.1099/mic.0.26455-0.
67. Brock TD, Brock KM, Belly RT, Weiss RL. 1972. *Sulfolobus*—new genus of sulfur-oxidizing bacteria living at low pH and high temperature. Arch Mikrobiol 84:54–68. https://doi.org/10.1007/BF00408082.
68. Frederiksen TM, Finster K. 2004. The transformation of inorganic sulfur compounds and the assimilation of organic and inorganic carbon by the sulfur disproportionating bacterium *Desulfocapsa sulfoexigens*. Antonie Van Leeuwenhoek 85:141–149. https://doi.org/10.1023/B:ANTO.0000020153.82679.f4.
69. Schink B. 1997. Energetics of syntrophic cooperation in methanogenic degradation. Microbiol Mol Biol Rev 61:262–280.
70. Kraemer SM. 2004. Iron oxide dissolution and solubility in the presence of siderophores. Aquat Sci 66:3–18. https://doi.org/10.1007/s00027-003-0690-5.
71. Roden EE, Zachara JM. 1996. Microbial reduction of crystalline iron(III) oxides: influence of oxide surface area and potential for cell growth. Environ Sci Technol 30:1618–1628. https://doi.org/10.1021/es9506216.
72. Livo KE, Kruse FA, Clark RN, Kokaly RF, Shanks W, III. 2007. Hydrothermally altered rock and hot-spring deposits at Yellowstone National Park characterized using airborne visible and infrared-spectroscopy data. Professional paper 1717. U.S. Geological Survey, Reston, VA.
73. Lengke MF, Tempel RN. 2003. Natural realgar and amorphous AsS oxidation kinetics. Geochim Cosmochim Acta 67:859–871. https://doi.org/10.1016/S0016-7037(02)01227-9.
74. Lengke MF, Sanpawanitchakit C, Tempel RN. 2009. The oxidation and dissolution of arsenic-bearing sulfides. Can Mineral 47:593–613. https://doi.org/10.3749/canmin.47.3.593.
75. Zhang JH, Zhang X, Ni YQ, Yang XJ, Li HY. 2007. Bioleaching of arsenic from medicinal realgar by pure and mixed cultures. Process Biochem 42:1265–1271. https://doi.org/10.1016/j.procbio.2007.05.021.
76. Tributsch H, Bennett JC. 1981. Semiconductor-electrochemical aspects of bacterial leaching. 1. Oxidation of metal sulfides with large energy gaps. J Chem Technol Biotechnol 31:565–577.
77. Tributsch H, Bennett JC. 1981. Semiconductor-electrochemical aspects of bacterial leaching. 2. Survey of rate-controlling sulfide properties. J Chem Technol Biotechnol 31:627–635.
78. Schippers A, Sand W. 1999. Bacterial leaching of metal sulfides proceeds by two indirect mechanisms via thiosulfate or via polysulfides and sulfur. Appl Environ Microbiol 65:319–321.
79. Schauder R, Muller E. 1993. Polysulfide as a possible substrate for sulfur-reducing bacteria. Arch Microbiol 160:377–382. https://doi.org/10.1007/BF00252224.
80. Schauder R, Kroger A. 1993. Bacterial sulfur respiration. Arch Microbiol 159:491–497. https://doi.org/10.1007/BF00249025.
81. Kamyshny A, Gun J, Rizkov D, Voitsekovski T, Lev O. 2007. Equilibrium distribution of polysulfide ions in aqueous solutions at different temperatures by rapid single phase derivatization. Environ Sci Technol 41:2395–2400. https://doi.org/10.1021/es062637+.
82. Segerer A, Neuner A, Kristjansson JK, Stetter KO. 1986. *Acidianus infernus* gen nov, sp nov, and *Acidianus brierleyi* comb nov—facultatively aerobic, extremely acidophilic thermophilic sulfur-metabolizing archaebacteria. Int J Syst Bacteriol 36:559–564. https://doi.org/10.1099/00207713-36-4-559.
83. He ZG, Zhong HF, Li YQ. 2004. *Acidianus tengchongensis* sp nov, a new species of acidothermophilic archaeon isolated from an acidothermal spring. Curr Microbiol 48:159–163. https://doi.org/10.1007/s00284-003-4155-9.
84. Plumb JJ, Haddad CM, Gibson JAE, Franzmann PD. 2007. *Acidianus sulfidivorans* sp nov, an extremely acidophilic, thermophilic archaeon isolated from a solfatara on Lihir Island, Papua New Guinea, and emendation of the genus description. Int J Syst Evol Microbiol 57:1418–1423. https://doi.org/10.1099/ijs.0.64846-0.
85. Fournier R, Weltman U, Counce D, White L, Janik C. 2002. Results of weekly chemical and isotopic monitoring of selected springs in Norris Geyser Basin, Yellowstone National Park during June-September, 1995. Open-file report 2002-344. U.S. Geological Survey, Reston, VA.
86. Hamilton TL, Boyd ES, Peters JW. 2011. Environmental constraints underpin the distribution and phylogenetic diversity of nifH in the Yellowstone geothermal complex. Microb Ecol 61:860–870. https://doi.org/10.1007/s00248-011-9824-9.
87. Hamilton TL, Peters JW, Skidmore ML, Boyd ES. 2013. Molecular evidence for an active endogenous microbiome beneath glacial ice. ISME J 7:1402–1412. https://doi.org/10.1038/ismej.2013.31.
88. Boyd ES, Cummings DE, Geesey GG. 2007. Mineralogy influences structure and diversity of bacterial communities associated with geological substrata in a pristine aquifer. Microb Ecol 54:170–182. https://doi.org/10.1007/s00248-006-9187-9.
89. Lovley DR, Phillips EJ. 1987. Rapid assay for microbially reducible ferric iron in aquatic sediments. Appl Environ Microbiol 53:1536–1540.
90. Fogo JK, Popowsky M. 1949. Spectrophotometric determination of hydrogen sulfide—methylene blue method. Anal Chem 21:732–734. https://doi.org/10.1021/ac60030a028.
91. Viollier E, Inglett PW, Hunter K, Roychoudhury AN, Van Cappellen P. 2000. The ferrozine method revisited: Fe(II)/Fe(III) determination in natural waters. Appl Geochem 15:785–790. https://doi.org/10.1016/S0883-2927(99)00097-9.
92. Cypionka H, Pfennig N. 1986. Growth yields of *Desulfotomaculum orientis* with hydrogen in chemostat culture. Arch Microbiol 143:396–399. https://doi.org/10.1007/BF00412808.
93. Johnson DL. 1971. Simultaneous determination of arsenate and phosphate in natural waters. Environ Sci Technol 5:411–414. https://doi.org/10.1021/es60052a005.

Downloaded from http://aem.asm.org/ on May 31, 2018 by MONTANA STATE UNIV AT BOZEMAN